Rom J Morphol Embryol 2017, 58(3):831–836

ORIGINAL PAPER

RJME
Romanian Journal of Morphology & Embryology
http://www.rjme.ro/

Effects of malalignment angle on the contact stress of knee prosthesis components, using finite element method

DANIELA TARNIŢĂ[1)], DAN MARIAN CALAFETEANU[1)], IONUŢ DANIEL GEONEA[1)], ALIN PETCU[1)], DĂNUŢ-NICOLAE TARNIŢĂ[2)]

[1)]*Department of Applied Mechanics, Faculty of Mechanics, University of Craiova, Romania*

[2)]*Department of Human Anatomy, Faculty of Medicine, University of Medicine and Pharmacy of Craiova, Romania*

Abstract

In this paper, the complex 3D virtual model of the prosthetic knee is obtained using embedded applications: DesignModeler and SpaceClaim under ANSYS Workbench 14.5 software package. A number of six cases of prosthetic knee joint assembly, depending on the malalignment angle, are developed. Stress maps and the values of the maximum von Mises stress on the three prosthesis components: polyethylene insert, tibial component and femoral component, for all studied prosthetic knee assemblies were obtained. The results show that as the malalignment angle increases, the values of von Mises stresses increase in all prosthesis components. The parameterized virtual models of the knee prosthesis components allow different changes in shape or dimensions, which can lead to the optimization of the implant and to the improvement of the prosthetic knee biomechanics.

Keywords: virtual knee prosthesis, finite element method, contact stress, malalignment.

Introduction

Virtual modeling and numerical simulation of human bones and joints have been addressed in several articles in the fields of biomechanics [1–8] and robotics [9–15]. From all the human joints, the knee joint is considered to be one of the most complex joints, taking into account the number of its components, their spatial geometry, their mechanical properties and their contact problems [5, 7, 12, 15–34]. In studies regarding the development of osteoarthritis [16–20], a disease which involves a degenerative process of cartilage in the knee joint, and regarding the role of the articular cartilage in the development of the osteoarthritis, the stress distributions on the cartilages and menisci, considering different angles on valgus and varus are presented. Varus angle is the angle made by the mechanical axis of tibia and femur in frontal plane. This angle is considered as normal from the physiological point of view, if its value is 176^{o}. Starting from the crossed knee sections obtained by computed tomography (CT) or magnetic resonance imaging (MRI), the 3D virtual models of normal and osteoarthritic human knee joint have been obtained and studied, by using finite element analysis (FEA) [16–20].

FEA is becoming one of the most important tools in orthopedic biomechanics, being used more and more to evaluate the stress and displacements, the biomechanical behavior of healthy bones and joints, of implant–bone assembly [1–8] or human joint–prosthesis/orthosis assemblies [21–34].

In order to study the influence of the malalignement angle on the contact stress of knee prosthesis components, in this study we have analyzed, by using FEA, the von Mises stress for the 3D model of the knee–prosthesis assembly corresponding to a set of six different values of malalignment angle, beginning from 176^{o} to 191^{o} with an increment equal to 3^{o}.

Methods

Geometric modeling

To design the virtual model of the knee prosthesis, we used the DesignModeler application, which is a preprocessor of ANSYS Workbench 15.07 software, often used in human biomechanics modeling and simulations [15, 17–19, 23, 28]. The virtual model of knee prosthesis was constructed starting from the shapes and dimensions of a well-known prosthesis, a Genesis II type knee prosthesis [23]. Beginning from the 3D virtual model of healthy knee joint [11], solids were built over the geometrical model of human knee, which was cut with profiles made in various planes, in order to respect the geometry. The three prosthesis components: polyethylene insert (P.I.), tibial prosthesis (T.P.) and femoral prosthesis (F.P.), were developed and presented in [23]. In Figure 1, the isometric views of designed knee prosthesis are presented.

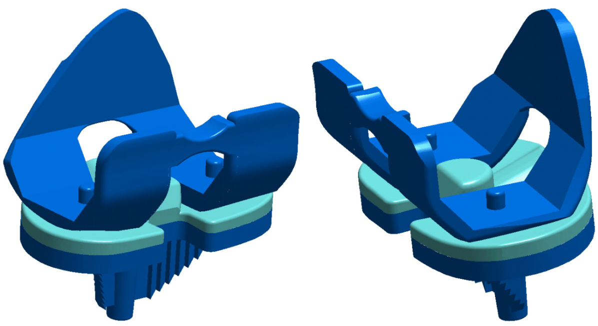

Figure 1 – *Two isometric views of virtual model of knee prosthesis.*

ISSN (print) 1220–0522 ISSN (online) 2066–8279

The six cases of malalignment of mechanical axis in frontal plane (varus) for prosthetic knee joint are presented in Figure 2.

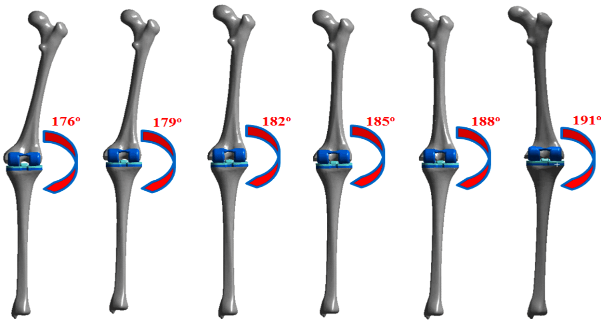

Figure 2 – *Six prosthetic knee joints with different malalignment angle.*

Mesh generation

To perform the numerical simulations of prosthetic knee joint, the following components that make up joint–prosthesis assembly have been considered: femur, tibia and the three components of the prosthesis: femoral component, tibial component and polyethylene insert. The meshing and the solution of the analyses stages, the correct positioning of components have been achieved in the simulation environment of ANSYS Workbench 15.07 application, which allows advanced modeling and discretization using FEA. The finite elements used in this analysis are hexahedral elements of Solid 186 type and tetrahedral elements of Solid 187 type, both being solid elements with middle nodes which are necessary for better approximation of results and for better accuracy. For an efficient mesh, we used elements with dimensions of 1 mm for the contacts areas, which present a maximum interest for FEA, dimension of 4 mm for the other regions of bones. In Figure 3, the mesh structure of the knee joint–prosthesis assembly is presented.

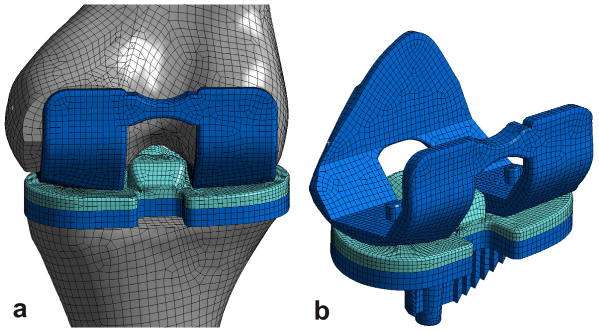

Figure 3 – *(a) Human knee joint with mounted prosthesis–Mesh of node and element network designed for the entire model; (b) Isometric view of nodes and elements network for the prosthesis.*

Boundary and constraints conditions for finite element analysis are:

▪ a "Remote Displacement" allows rotation of the ankle around the *Y* axis; all other displacements and rotation movements have been set as 0; degree of freedom = 1 (Figure 4a);

▪ on the proximal head of the femur bone, a "Remote Displacement" that allows offset *Z* and Rot *Y* around the femur (the yellow area) and movement of the hip is applied (Figure 4b);

▪ for hip joint, rotation movement around *Y* axis and translation on *Z* axis are established; translations on *X* and *Y* axis, respectively rotations around *X* and *Z* axis are considered equal to 0; degree of freedom = 2;

▪ on the proximal head of the femur bone, a distributed force of 2400 N is applied on the -*Z* axis direction (Figure 4c).

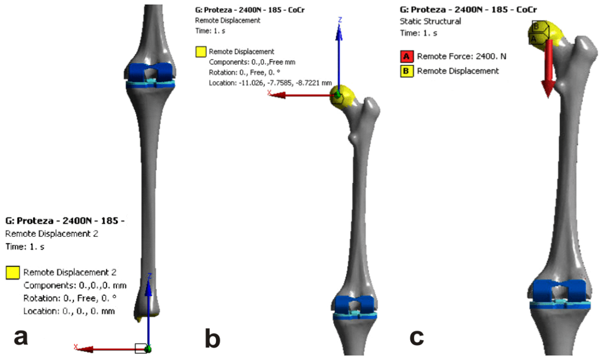

Figure 4 – *(a–c) Constraints and boundary conditions.*

Results

Using ANSYS Workbench 15.07 software, the numerical simulations and finite element method (FEM) analyses were processed for six cases of varus angle (from 176° to 191° with a step of 3°) of knee joint–prosthesis assembly, considering a loading force equal to 2400 N, a force equal to three times the medium body weight (BW). A total number of 298 959 nodes and 92 070 elements were obtained for analysis of the joint–prosthesis model with a varus angle equal to 176° (Table 1). For the other five cases, the dimensions of the networks are similar, but they present a different number of nodes and elements caused by the changes of contact geometry (Table 2).

The properties of materials for human knee components and for prosthesis components necessary for the FEM analysis using ANSYS software are presented in Table 3.

Table 1 – *The network of nodes and elements*

Component	Nodes	Elements
Femur	129 059	40 491
Tibia	72 285	22 250
Femoral component	28 680	8605
Tibial component	22 979	7295
Polyethylene component	45 956	13 429
Total	*298 959*	*92 070*

Table 2 – *The network of nodes and elements for all six cases*

	176°	179°	182°	185°	188°	191°
No. of nodes	298 959	298 696	296 696	294 352	291 291	289 620
No. of elements	92 070	92 687	92 131	91 448	90 137	89 875

Table 3 – *Materials properties for knee–prosthesis assembly [15, 30]*

Component	Young's modulus [MPa]	Poisson's ratio
Femur	17 600	0.3
Tibia	12 500	0.3
Femoral component	210 000	0.3
Tibial component	210 000	0.3
Polyethylene component	1100	0.42

Von Mises stresses maps obtained for the six studied cases are presented in Figures 5–10. The images represent Top and Bottom views of each component for all the six studied cases. Red color represents the highest stress, while the dark blue color represents the lowest stress (0 value).

The maximum values of von Mises stresses developed in the prosthesis components: polyethylene insert (P.I.), tibial prosthesis (T.P.) and femoral prosthesis (F.P.) were extracted for the studied case and presented in Table 4. The values are expressed in MPa (1 MPa is the measure unit used for stresses; 1 MPa = 1 N/mm^2 = 10^6 Pa).

Table 4 – ***Von Mises stress maximum values corresponding to a force equal to 2400 N***

Cases	Stress P.I. [MPa]	Stress T.P. [MPa]	Stress F.P. [MPa]
176°	33.12	31.03	32.84
179°	34.27	31.75	33.61
182°	35.31	32.41	34.14
185°	36.19	33.19	35.02
188°	36.94	34.14	35.63
191°	37.24	35.27	36.29

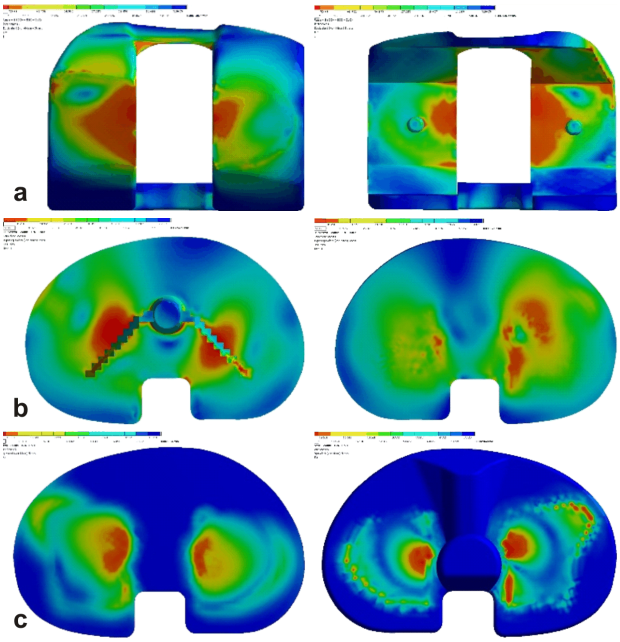

Figure 5 – ***Von Mises stress distribution (bottom view – left; top view – right) for varus angle of prosthetic knee joint – 176°: (a) Femoral component; (b) Tibial component; (c) Polyethylene insert.***

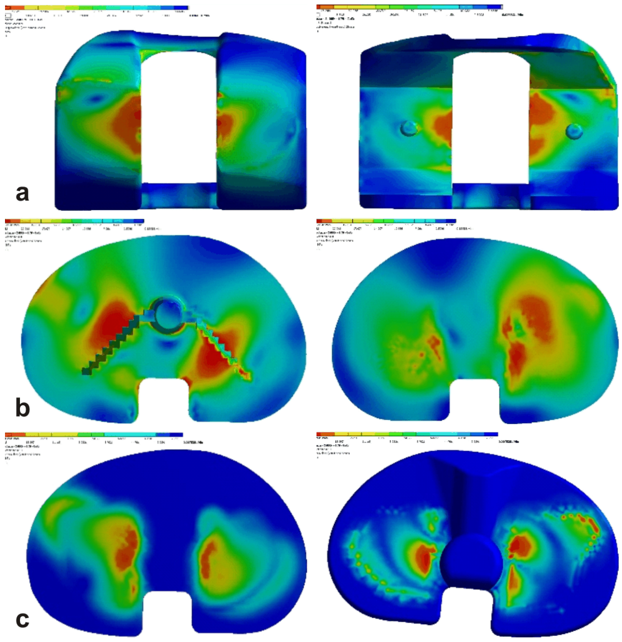

Figure 6 – ***Von Mises stress distribution (bottom view – left; top view – right) for varus angle of prosthetic knee joint – 179°: (a) Femoral component; (b) Tibial component; (c) Polyethylene insert.***

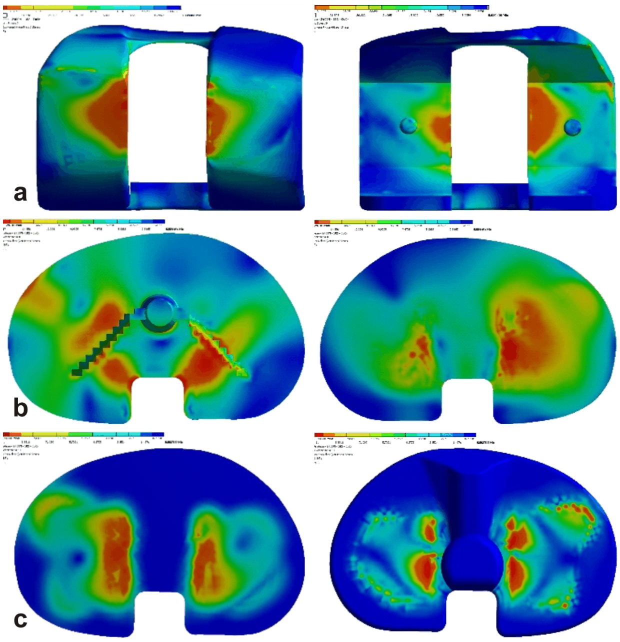

Figure 7 – ***Von Mises stress distribution (bottom view – left; top view – right) for varus angle of prosthetic knee joint – 182°: (a) Femoral component; (b) Tibial component; (c) Polyethylene insert.***

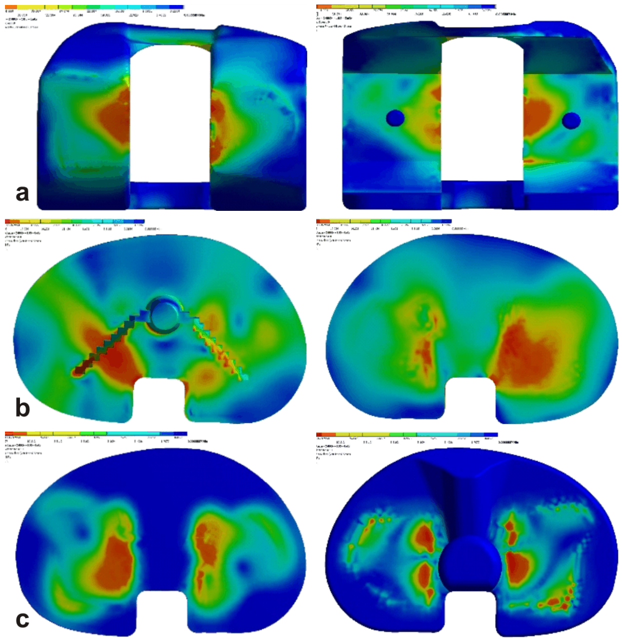

Figure 8 – ***Von Mises stress distribution (bottom view – left; top view – right) for varus angle of prosthetic knee joint – 185°: (a) Femoral component; (b) Tibial component; (c) Polyethylene insert.***

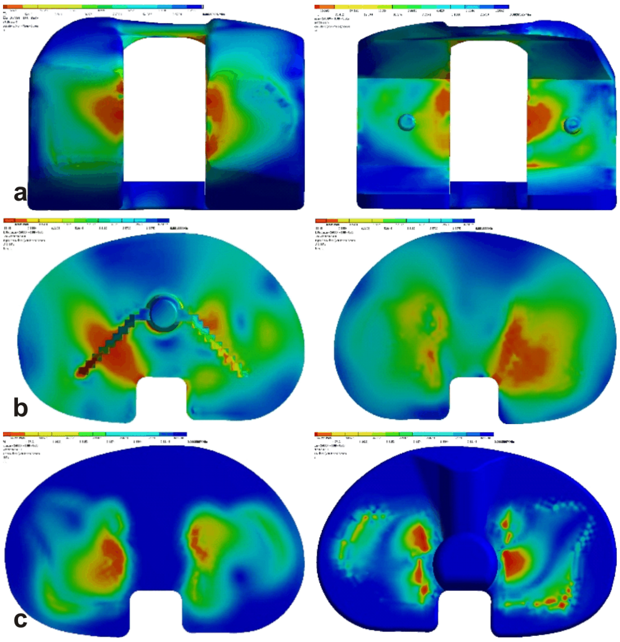

Figure 9 – *Von Mises stress distribution (bottom view – left; top view – right) for varus angle of prosthetic knee joint – 188°: (a) Femoral component; (b) Tibial component; (c) Polyethylene insert.*

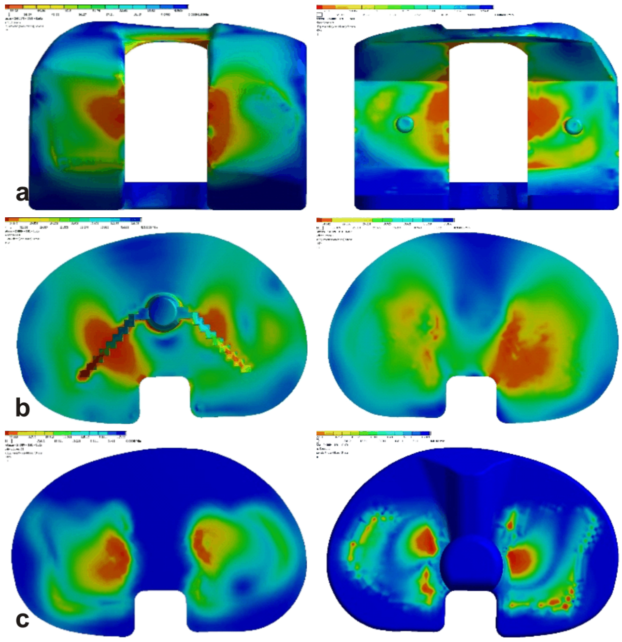

Figure 10 – *Von Mises stress distribution (bottom view – left; top view – right) for varus angle of prosthetic knee joint – 191°: (a) Femoral component; (b) Tibial component; (c) Polyethylene insert.*

Analyzing the results obtained by numerical simulations, presented in Table 4, it is noticed that, as the angle of inclination in varus increases, the values of von Mises stresses increase in all prosthesis components. In all cases, the stress values are similar, with small differences, but we can conclude that the bigger values are developed on polyethylene insert, followed by the values developed on femoral component and, respectively, on the tibial component. Increased varus frontal plane tibiofemoral alignment leads to an increase of the mechanical loading on the medial compartment of the knee. The variation of maximum stress values function of varus angle for all three prosthesis components are shown in Figure 11, while in Figure 12 maximum stress values for the three prosthesis components are presented.

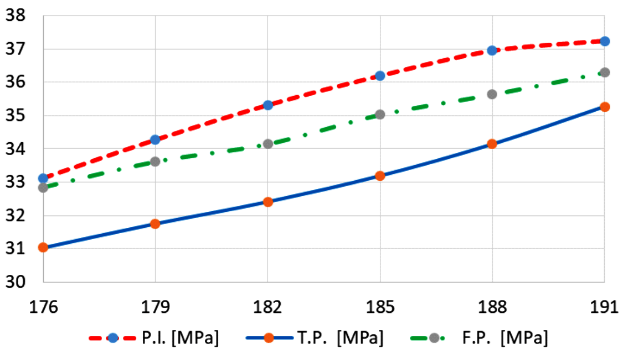

Figure 11 – *Diagram of maximum stress values function of varus angle. P.I.: Polyethylene insert; T.P.: Tibial prosthesis; F.P.: Femoral prosthesis.*

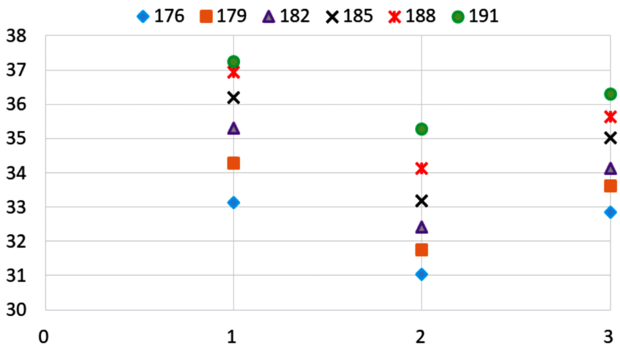

Figure 12 – *Maximum stress values [MPa] for the prosthesis components: 1 – P.I.; 2 – T.P.; 3 – F.P.*

Discussion

Many studies have focused on the experimental or numerical evaluation of these loads in normal, osteoarthritic or prosthetic knee joint [28–42]. A very important aspect in order to study the behavior of the prosthetic knee components is the correct evaluation of the tibiofemoral loads. In previous studies, force values equivalent to three to four times BW have been used in most biomechanical tests evaluating prosthetic knee joints [31–33]. The tibiofemoral forces in [34] were close to four times BW during level walking and more than eight times BW during downhill walking. Morisson considered the knee joint loads during level walking as three times BW [35], while Collins [36] calculated them using an optimization method and concluded that they range from 3.9 to 6.0 times BW. Jefferson *et al.* [39] found that the maximum tibiofemoral loads are up to 6.3 times BW, while Wyss *et al.* [40] report values ranging from 2.5 to 5 times BW. In order to improve the design of total knee replacements, it is necessary to adopt higher tibiofemoral loads than the bodyweight (BW) [34]. In this study, we will consider a compressive force equal to 2400 N, equivalent of three times BW of a person with normal weight of 800 N.

Contact area is a very important parameter, which influences the contact stresses values on joint stress.

The reported average contact area of a natural knee joint ranges from 765 mm^2 to 1150 mm^2 [13, 34, 41, 42]. The contact area of most total knee prostheses is between 80 and 300 mm^2 depending on the load, flexion angle and design leading to contact stresses on the P.I. as high as 60 MPa [34, 42]. Contact areas varied from line-shaped to bilateral circular or elliptical shapes [42]. In this paper, the studied prosthesis is a Genesis II type one, with a contact area equal to about 95 mm^2 for 0^o in flexion. The studies reveal that the contact area for this prosthesis type presents small variations for different flexion angles [41]. This area is about 105 mm^2 for 60^o flexion angle and about 110 mm^2 for 15^o flexion angle. In consequence, for this type of prosthesis, the contact stresses have higher values for orthostatic position (0^o in flexion) and, generally, they have a small variation during the flexion movement. Therefore, an analyze of the von Mises stresses developed in the 3D virtual prosthesis for 0^o in flexion will cover all other cases corresponding to different flexion angles.

The maximum values of contact stresses, higher than 30 MPa, reported in Table 4, were recorded on small areas (approximately 5–10 mm^2), relative to the entire contact surface, which is 95–110 mm^2.

The average values of contact stress reported on the entire contact area have values comprised in the interval (22–25) MPa, but, function of the stress values ranges, the distribution of the contact stresses is: on a about 15–20 mm^2 area, the contact stresses range in the interval (0–10) MPa, on an area of about 15–20 mm^2 the contact stresses range in the interval (10–15) MPa, on 15–20 mm^2 the contact stresses range in (15–20) MPa, and on about 30–35 mm^2 the contact stresses range in the interval (20–25) Mpa. The results and the distribution of the contact stresses values on the contact area are similar with those obtained by Szivek *et al.* [41]. The contact stress patterns collected at 24^oC were different than those collected at physiological temperature (*i.e.*, 37^oC) [41]. In general, at the higher temperature, larger contact areas and lower stresses were reported by Szivek *et al.* [41].

In this study, the results are limited to the static loading condition. Therefore, future research works will examine the behavior of the prosthetic knee under dynamic loading situation, and the effect of flexion angle during walking, on the actual implant geometries and on the contact stresses. A larger contact area of approximately 350–400 mm^2 is necessary to avoid stresses to the polyethylene inlay that are above the yield point of 20 MPa [34]. This contact area should be maintained throughout a flexion range of 0° to 60° to accommodate the high loads developed in some daily activities, as downstairs [34].

Conclusions

In this paper, starting from the 3D virtual model of the human knee joint and from the 3D virtual models of the components of an existent knee prosthesis, often used in total knee arthroplasty, by using ANSYS Workbench 15.07 software, the stress maps are obtained for six analyzed knee-prosthesis assemblies. Given a realistic model for prosthesis components and appropriate boundary conditions, this approach can accurately predict contact stresses. The results obtained in this study are very important for surgeons and researchers to develop optimized devices for total joints replacement. The parameterized virtual models of the knee prosthesis allow different changes in shape or dimensions, which means an advantage which can lead to the implant optimization and to the knee biomechanics improvement.

Conflict of interests

The authors declare no conflict of interests.

Acknowledgments

The authors are grateful to Dr. Eng. Marius Ionel Catană, for his assistance with the numerical simulations.

References

[1] Schileo E, Taddei F, Malandrino A, Cristofolini L, Viceconti M. Subject-specific finite element models can accurately predict strain levels in long bones. J Biomech, 2007, 40(13):2982–2989.

[2] Tarniţă D, Tarniţă DN, Popa D, Grecu D, Tarniţă R, Niculescu D, Cismaru F. Numerical simulations of human tibia osteosynthesis using modular plates based on Nitinol staples. Rom J Morphol Embryol, 2010, 51(1):145–150.

[3] Completo A, Fonseca F, Simões JA. Experimental validation of intact and implanted distal femur finite element models. J Biomech, 2007, 40(11):2467–2476.

[4] Tarniţă D, Tarniţă DN, Bîzdoacă N, Tarniţă C, Berceanu C, Boborelu C. Modular adaptive bone plate for humerus bone osteosynthesis. Rom J Morphol Embryol, 2009, 50(3):447–452.

[5] Donahue TL, Hull ML, Rashid MM, Jacobs CR. A finite element model of the human knee joint for the study of tibio-femoral contact. J Biomech Eng, 2002, 124(3):273–280.

[6] Tarniţă D, Boborelu C, Popa D, Tarniţă C, Rusu L. The three-dimensional modeling of the complex virtual human elbow joint. Rom J Morphol Embryol, 2010, 51(3):489–495.

[7] Penrose JM, Holt GM, Beaugonin M, Hose DR. Development of an accurate three-dimensional finite element knee model. Comput Methods Biomech Biomed Eng, 2002, 5(4):291–300.

[8] Tarnita D, Tarnita DN, Tarnita R, Berceanu C, Cismaru F. Modular adaptive bone plate connected by Nitinol staple [Modulare Knochenplatte von Nitinol Klammern verbunden]. Materialwiss Werkst, 2010, 41(12):1070–1080.

[9] Geonea ID, Alexandru C, Margine A, Ungureanu A. Design and simulation of a single DOF human-like leg mechanism. Olaru A (ed), Appl Mech Mater, 2013, 332:491–496.

[10] Gherman B, Pisla D, Vaida C, Plitea N. On workspace and accuracy evaluation of a parallel robot for needle placement procedures. Proc Rom Acad A Math Phys Tech Sci Inform Sci, 2013, 17(4):344–351.

[11] Alexandru C. Optimal design of the mechanical systems using parametric technique & MBS (multi-body systems) software. Fan W (ed), Adv Mater Res, 2012, 463–464:1129–1132.

[12] Tarnita D, Tarnita DN, Bizdoaca N, Popa D. Contributions on the dynamic simulation of the virtual model of the human knee joint [Beiträge zur dynamischen Simulation des virtuellen Modells des menschlichen Kniegelenks]. Materialwiss Werkst, 2009, 40(1–2):73–81.

[13] Pisla D, Plitea N, Gherman BG, Vaida C, Pisla A, Suciu M. Kinematics and design of a 5-DOF parallel robot used in minimally invasive surgery. In: Lenarčič J, Stanišić MM (eds). Advances in robot kinematics: motion in man and machine. Springer Netherlands, Springer Science + Business Media B.V., 2010, 99–106.

[14] Dumitru N, Copilusi C, Geonea I, Tarnita D, Dumitrache I. Dynamic analysis of an exoskeleton new ankle joint mechanism. In: Flores P, Viadero F (eds). New trends in mechanism and machine science: from fundamentals to industrial applications. Book Series “Mechanisms and Machine Science”, vol. 24, Springer International Publishing, Switzerland, 2015, 709–717.

[15] Tarnita D, Catana M, Tarnita DN. Contributions on the modeling and simulation of the human knee joint with applications to the robotic structures. In: Rodić A, Pisla D, Bleuler H (eds). New trends in medical and service robotics: challenges and

solutions. Book Series "Mechanisms and Machine Science", vol. 20, Springer International Publishing, Switzerland, 2014, 283–297.
[16] Bae JY, Park KS, Seon JK, Kwak DS, Jeon I, Song EK. Biomechanical analysis of the effects of medial meniscectomy on degenerative osteoarthritis. Med Biol Eng Comput, 2012, 50(1):53–60.
[17] Yang NH. The effect of the frontal plane tibiofemoral angle on the contact stress and strain at the knee joint. Mechanical Engineering Dissertations, Department of Mechanical and Industrial Engineering, College of Engineering, Northeastern University, Boston, Massachusetts, USA, 2009.
[18] Vidal A, Lesso R, Rodríguez R, García S, Daza L. Analysis, simulation and prediction of contact stresses in articular cartilage of the knee joint. WIT Transactions on Biomedicine and Health, Modelling in Medicine and Biology VII, Brebbia CA (ed), 2007, 12:55–64.
[19] Tarnita D, Tarnita D, Bolcu D. Orthopaedic modular implants based on shape memory alloys. In: Fazel-Rezai R (ed). Biomedical engineering – from theory to applications. InTech, Viena, 2011, 431–468.
[20] Kubíček M, Florian Z. Stress strain analysis of knee joint. Eng Mech, 2009, 16(5):315–322.
[21] Godest AC, de Cloke CS, Taylor M, Gregson PJ, Keane AJ, Sathasivan S, Walker PS. A computational model for the prediction of total knee replacement kinematics in the sagittal plane. J Biomech, 2000, 33(4):435–442.
[22] Yang RS, Lin HJ. Contact stress on polyethylene components of a new rotating hinge with a spherical contact surface. Clin Biomech (Bristol, Avon), 2001, 16(6):540–546.
[23] Tarnita D, Calafeteanu D, Catana, M, Geonea I, Tarnita D. Development of a three-dimensional finite element knee prosthesis model. Dumitru I (ed), Appl Mech Mater, 2016, 822:150–155.
[24] Halloran JP, Petrella AJ, Rullkoetter PJ. Explicit finite element modeling of total knee replacement mechanics. J Biomech, 2004, 38(2):323–331.
[25] Liau JJ, Cheng CK, Huang CH, Lo WH. The effect of malalignment on stresses in polyethylene component of total knee prostheses – a finite element analysis. Clin Biomech (Bristol, Avon), 2002, 17(2):140–146.
[26] Taylor M, Barrett DS. Explicit finite element simulation of eccentric loading in total knee replacement. Clin Orthop Relat Res, 2003, 414:162–171.
[27] Godest AC, Beaugonin M, Haug E, Taylor M, Gregson PJ. Simulation of a knee joint replacement during a gait cycle using explicit finite element analysis. J Biomech, 2002, 35(2): 267–275.
[28] Calafeteanu D, Tarnita D, Catana M, Tarnita D. Influences of varus tilt on the stresses in human prosthetic knee joint. Tarnita D (ed), Appl Mech Mater, 2016, 823:143–148.
[29] Harrysson OL, Hosni YA, Nayfeh JF. Custom-designed orthopedic implants evaluated using finite element analysis of patient-specific computed tomography data: femoral-component case study. BMC Musculoskelet Disord, 2007, 8:91.
[30] Villa T, Migliavacca F, Gastaldi D, Colombo M, Pietrabissa R. Contact stresses and fatigue life in a knee prosthesis: comparison between *in vitro* measurements and computational simulations. J Biomech, 2004, 37(1):45–53.
[31] Collier JP, Mayor MB, McNamara JL, Surprenant VA, Jensen RE. Analysis of the failure of 122 polyethylene inserts from uncemented tibial knee components. Clin Orthop Relat Res, 1991, 273:232–242.
[32] Walker PS. Requirements for successful total knee replacements. Design considerations. Orthop Clin North Am, 1989, 20(1):15–29.
[33] McNamara JL, Collier JP, Mayor MB, Jensen RE. A comparison of contact pressures in tibial and patellar total knee components before and after service *in vivo*. Clin Orthop Relat Res, 1994, 299:104–113.
[34] Kuster MS, Wood GA, Stachowiak GW, Gächter A. Joint load considerations in total knee replacement. J Bone Joint Surg Br, 1997, 79(1):109–113.
[35] Morrison JB. The mechanics of the knee joint in relation to normal walking. J Biomech, 1970, 3(1):51–61.
[36] Collins JJ. The redundant nature of locomotor optimization laws. J Biomech, 1995, 28(3):251–267.
[37] Tarniţă D. Wearable sensors used for human gait analysis. Rom J Morphol Embryol, 2016, 57(2):373–382.
[38] Tarniţă D, Catană M, Tarniţă DN. Experimental measurement of flexion–extension movement in normal and osteoarthritic human knee. Rom J Morphol Embryol, 2013, 54(2):309–313.
[39] Jefferson RJ, Collins JJ, Whittle MW, Radin EL, O'Connor JJ. The role of the quadriceps in controlling impulsive forces around heel strike. Proc Inst Mech Eng H, 1990, 204(1):21–28.
[40] Wyss UP, Costigan PA, Li J, Olney SJ, Zee BC, Cooke TDV. Bone-on-bone forces at the knee joint during walking and stairclimbing. J Biomech, 1994, 27(6):819.
[41] Szivek JA, Anderson PL, Benjamin JB. Average and peak contact stress distribution evaluation of total knee arthroplasties. J Arthroplasty, 1996, 11(8):952–963.
[42] Postak PD, Heim CS, Greenwald AS. Tibial plateau surface stress in TKA: a factor influencing polymer damage. Series VI, American Academy of Orthopaedic Surgeons (AAOS) Conference, New Orleans, 1994.

Corresponding author
Dănuţ-Nicolae Tarniţă, Professor, MD, PhD, Department of Human Anatomy, Faculty of Medicine, University of Medicine and Pharmacy of Craiova, 2 Petru Rareş Street, 200349 Craiova, Romania; Phone +40722–282 229, e-mail: dan_tarnita@yahoo.com

Received: October 18, 2016

Accepted: October 1, 2017